PERGAMON

European Journal of Cancer 37 (2001) 520–530

European Journal of Cancer

www.ejconline.com

Effects of a novel synthetic retinoid on malignant glioma *in vitro*: inhibition of cell proliferation, induction of apoptosis and differentiation

S.L. Costa [a], E. Paillaud [a], C. Fages [a], C. Rochette-Egly [b], J.L. Plassat [b], H. Jouault [c], A. Perzelova [d], M. Tardy [a,*]

[a] *INSERM U-421, Faculté de médicine, 8 rue du Général Sarrail, 94010 Créteil cedex, France*
[b] *Institut de Génétique et Biologie Moléculaire et Cellulaire, Illkirch, France*
[c] *Service d'Hématologie Biologique, Hôpital Henri Mondor, Créteil, France*
[d] *School of Medicine, Comenius University, Bratislava, Slovakia*

Received 23 June 2000; received in revised form 17 October 2000; accepted 18 October 2000

Abstract

Among six synthetic retinoids tested, the retinoid 6-[3-(1-adamantyl)-4-hydroxyphenyl]-2-naphthalene carboxylic acid (CD437) was highly efficient in inducing growth inhibition of 8MG-BA and GL-15 human glioblastoma cell lines, with growth arrest at the S phase of the cell cycle. CD 437 also induced apoptosis in these cells, with 8MG-BA being the most sensitive. In these cells, induction of apoptosis by CD437 has been related to the downregulation of Bcl-2 expression and to CPP32 activation, but not to p53 expression. The remaining non-apoptotic cells presented a morphological pattern of astroglial differentiation with overexpression of glial fibrillary acidic protein (GFAP) and glutamine synthetase (GS). The mechanism of action of CD437, originally developed as a RARγ agonist, is not yet elucidated. However, our results suggest that it acts through an increase of the expression of retinoid-inducible genes, such as RARβ2 and/or RARα2.

Keywords: Retinoids; CD437; Glioma; Apoptosis; Differentiation

1. Introduction

Therapeutic studies indicated recently that patients with malignant glioma and treated with all-*trans* retinoic acid (t-RA), showed positive, but heterogeneous effects [1]. Inhibition of cell proliferation by high t-RA concentrations was demonstrated in glioma cell lines [2], but these effects were only partial and transitory. Retinoids are a class of natural and synthetic vitamin A analogues that play a central role in the control of cell growth and differentiation of normal and malignant cell types [3,4]. Many of the biological and molecular effects of retinoids are mediated by two types of nuclear receptors, the retinoid acid receptors (RARs) and retinoid X receptors (RXRs), each of which is encoded by three genes designed α, β and γ [5]. This discovery raised the hope that retinoids whose receptor selectivity is restricted to specific RAR or RXR subtypes may be more effective and might be adopted for cancer therapy [6]. Recently, 6-[3-(1-adamantyl-4-hydroxyphenyl]-2-naphthalene carboxylic acid (CD437), originally developed as a RARγ agonist, was reported to induce apoptosis in human melanoma, breast carcinoma, lung carcinoma and promyelocytic leukaemia cell lines [7–9]. In contrast to t-RA, this novel compound did not appear to require activation of RARs or RXRs to exert its effect [10]. However, the contribution of RARγ activation to its activity cannot be completely excluded, since RARγ-selective retinoid agonists were reported to inhibit cell growth [11]. Importantly, the growth inhibitory and apoptosis-inducing effects of CD437 were observed in t-RA-refractory breast cancer and leukaemia cell lines [10,11], indicating that it may represent a novel class of compound suitable for the treatment of t-RA-resistant cancers, and may be effective for glioma therapy.

* Corresponding author. Tel.: +33-1-4981-3624; fax: +33-1-4981-3709.
E-mail address: tardy@im3.inserm.fr (M. Tardy).

0959-8049/01/$ - see front matter
PII: S0959-8049(00)00430-5

Therefore, in this study we tested the effect of synthetic retinoids on the growth of two human glioblastoma cell lines (GL-15 and 8MG-BA). We focused the present study on the effects of CD437.

2. Materials and methods

2.1. Cell lines and culture

The GL-15 [12] and 8MG-BA [13] cell lines were derived from human multiforme glioblastomas. Cells were grown until confluence in cell culture dishes (Corning) in Dulbecco's Modified Eagle's Medium (DMEM)/MEM (v/v) medium (Boehringer, Mannheim, Germany), supplemented with 100 UI/ml penicillin G, 100 μg/ml streptomycin, 7 mM glucose, 2 mM L-glutamine, 0.011 g/l pyruvate, and 10% fetal calf serum. They were both around 100 passages from their primary tumours.

2.2. Retinoids

The retinoid 6-[3-(1-adamantyl)-4-hydroxyphenyl]-2-naphthalene carboxylic acid (CD437), CD336, CD2019, CD2809, CD666, CD2325 were synthesised by GALDERMA Research and Development (Sophia Antipolis, France). All retinoids were dissolved in dimenthylsulphoxide (DMSO) at a concentration of 10 mM and were stored in the dark at −20°C.

2.3. Cell proliferation assay

Proliferation was studied by [^{3}H]-thymidine incorporation. [^{3}H]-thymidine (1 μCi/ml) was added to triplicate cultures 5 h before the end of the experiments. Cells were lysed in the presence of 0.1% sodium dodecyl sulphate (SDS) and labelled DNA was precipitated with 10% trichloroacetic acid (TCA) for 45 min on ice, and retained on GF/A filters (Whatman, UK). Radioactivity of the TCA insoluble fraction was evaluated in a β-scintillation counter and expressed as percentage of control incorporation ± standard deviation (S.D.).

Alternatively, growth curves and cellular viability was assessed by Trypan Blue (Sigma, St Louis, MO, USA) staining of both floating and adherent cells treated with 1 μM CD437 for different times. Adherent cells were harvested by trypsinisation, grouped with floating cells, then centrifuged at 1300*g*. Cells were stained with trypan blue at a final concentration of 0.1% (v/v). Four replicate wells were used for each analysis. The number of viable and non-viable cells were determined by counting 50 μl of cell suspension for each experiment in a Malacez chamber.

2.4. Cell cycle analysis

Flow cytometry analysis of DNA content was performed to assess the cell cycle phase distribution after CD437 (1 μM) was added to logarithmically growing glioblastoma cells. Cells were harvested by trypsinisation at various times and stained with propidium iodide using a DNA Con3 Staining Kit (Consults, Rivolta de Torino, Italy) according to the manufacturer's instructions. Flow cytometry analysis was performed on a Coulter Epics XL cytometer (Beckman-Coulter). The computer program Multicycle Software from Phoenix Flow Systems (San Diego, CA, USA) was used to generate histograms, and to determine the cell cycle phase distribution.

2.5. Apoptosis detection

Two protocols were adopted to identify apoptosis in glioblastoma cells treated with CD437: Annexin V labelling and nuclear staining. The analysis of phosphatidylserine on the outer leaflet of apoptotic cell-membranes was performed using Annexin-V-Alexa^{TM} 589 Kit, according to instructions of the manufacturer. After fixation of adherent cells with cold methanol, nuclear condensation and/or fragmentation was detected by staining cells for 5 min with the fluorescent dye Hoechst 33258 (Sigma) at 5 μg/ml in phosphate-buffered solution (PBS). The apoptotic index represents the percentage of fragmented nuclei and was determined on a microscopic field of at least 500 cells/experimental point.

2.6. Immunocytochemistry

Control and CD437-treated cells were rinsed twice with PBS, fixed with cold methanol at −20°C and incubated with mouse monoclonal antivimentin (clone 3B4, 1/200, Boehringer) or rabbit polyclonal anti-GFAP (1/200, DAKO, Denmark), then incubated with fluorecein isothiocyanate (FITC) (Boehringer, Mannheim, Germany) or tetramethylahodamine isothiocyanate (TRITC) (Biomakor-3359, 1/400, Israel) conjugated rabbit anti-mouse or goat antirabbit antibodies, respectively. The cells were then analysed by fluorescent microscopy.

2.6.1. Measurement of CPP32-like caspase activity

For determination of DEVD-amc hydrolytic activity, cells were plated on 3.5-cm diameter dishes 1 day before treatment. Confluent cells in triplicate were exposed to 1 μM CD437 for 3, 6, 9 or 24 h. Cells were rinsed twice with PBS and harvested with lysis buffer (10 mM HEPES, 5 mM ethylene diamine tetra acetic acid (EDTA), 1.5 $MgCl_2$, 10 mM KCl, 0.1% (v/v) Triton X-100, 0.5 mM dithiothreitol (DTT), 0.2 mM phenylmethylsulphonylfluoride (PMSF), 5 μl/ml protease inhibitor cocktail (Sigma, St Louis, MO, USA). After

incubation on ice for 20 min and centrifugation at 12 000*g* for 20 min, the supernatants were collected and protein concentration was determined with the Protein Assay Kit (Bio-Rad, Hercules, CA, USA). Aliquots (40 μg) were used for CPP32-caspase activity assay using the Ac-DEVD-AFA fluorogenic substrate (AFC) and the CPP32 inhibitor Z-DEVD-CHO (BIOMOL, PA, USA) at final concentrations of 2 nM. After 3 h at 37°C, fluorescence was quantified (excitation 400 nm, emission 505 nm) in a Perkin-Elmer LS50 spectrofluorimeter. Optimal amounts of lysates and optimal durations of assay were taken from linear portions of standards curves. One unit of caspase activity was taken as one fluorescence unit (at a slit width of 10 nm) per 3 h incubation with substrate.

2.6.2. Western immunoblotting

Cells were rinsed twice with PBS and harvested in lysis buffer 2% (w/v) SDS, 62.5 mM Tris–HCl, pH 6.8, 2 mM EDTA, 2 mM ethylene glycol-tetra acetic acid (EGTA), 4 M Urea, 0.5% (v/v) Triton X-100, 1% Nonidet P-40 (NP40), 1 mM PMSF, 0.5 mM sodium vanadate, 1 μg/ml aprotinin, 1 μg/ml leupeptin, 0.1 mM iodoacetamin, 1 mM benzamidine, 10 mM N-ethylmaleimide and 10 mU/ml α2-macroglobulin). Protein concentration was determined with the Protein Assay Kit (Bio-Rad, Hercules, CA, USA). For vimentin, GFAP and GS analyses, 10 μg of total protein were resolved by discontinuous SDS polyacrylamide gel electrophoresis (PAGE) with a 5% (v/v) acrylamide stacking gel and a 10% (v/v) acrylamide separating gel, and electroblotted onto nitrocellulose membranes (Bio-Rad, USA). Membranes were incubated for 1 h in blocking buffer 5% (w/v) bovine serum albumin (BSA), 0.1% (v/v) Tween 20 in TBS (20 mM Tris-base, 137 mM sodium chloride 1 M hydrochloric acid, pH 7.6), washed three times with TBS containing 0.1% (v/v) Tween 20 (TBS-T), then incubated with rabbit polyclonal anti-GFAP (DAKO, Denmark), mouse monoclonal antibody antivimentin (clone V9, Boehinger, Mannheim, Germany) or mouse monoclonal antibody anti-GS [32]

For Bcl-2 and Bax analysis, proteins (40 μg) were resolved by SDS-PAGE using a 5% (v/v) acrylamide stacking gel and a 12% (v/v) acrylamide separating gel, and electroblotted as above, then incubated with mouse monoclonal antibodies against Bcl-2 (clone AC21, Santa Cruz) or Bax (clone B9, Santa Cruz) in this buffer. After three washes with TBS-T, the membranes were incubated in the same buffer containing horseradish peroxidase conjugated sheep antirabbit or antimouse immunoglobulins. After three washes with TBS-T, membranes were developed using enhanced chemiluminescence according to the manufacturer's instructions (Amersham, Life Sciences, UK), and exposed to Hyperfilm MP. Developed films were analysed by scanning densitometry.

2.6.3. Polymerase chain reaction (PCR)

Total RNA was extracted from 8MG-BA and GL-15 cells using the guanidium thiocyanate method [35]. The amount of RNA used for RT-PCR in each reaction (2 μg) was normalised with 36B4 transcripts, which are unresponsive to retinoid treatment. The RT-PCR primers were as follows: *RARα2* 5′-AACCCCTTCCTA-GTGGTGGA-3′ (forward) and 5′TTGCTCCAGGA-GAAAGGGGCT-3′ (reverse); *RARβ2* 5′-GAATGG-CAGCATCGGCACAC-3′ (forward) and 5′-GCTCTC-TGTGCATTCTTGCT-3′ (reverse); *RARγ1* 3′-CTCC-GCCTTTCGAGATGCTG-3′ (forward) and 5′-TTG-CCCAGCTGGCAGAGCGA-3′ (reverse); *RARγ2* 5′-TGTTTCGCCGGACTTGAATC-3′ (forward) and 5′-TTGCCCAGCTGGCAGAGCGA-3′ (reverse); *β-Actin* 5′-GCGCTCGTCGTCGACAACGG-3′ (forward) and 5′-CAGCCTGGATAGCAACGTA-3′ (reverse). Aliquots were electrophoresed on a 1.5% agarose gel and samples were transferred onto Hybond-N membranes (Amersham). The RT-PCR blots were probed with end-labelled oligonucleotides probes, and analysed by autoradiography.

2.6.4. Detection of TP53 *mutation*

Characterisation of *TP53* gene mutation in 8MG-BA and GL-15 cell lines was performed by sequencing exons 2–10 and the intron–exons junctions in both

Table 1
Retinoid selectivity

Retinoid	RAR selectivity
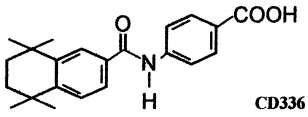 CD336	RARα
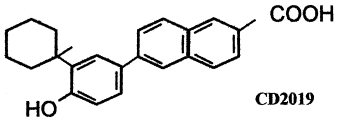 CD2019	RARβ
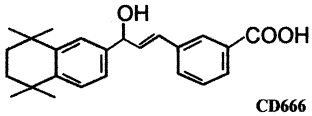 CD666	RARγ
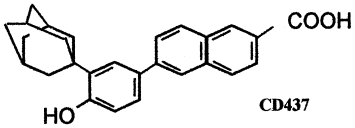 CD437	RARγ
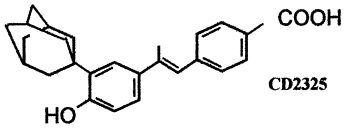 CD2325	RARγ
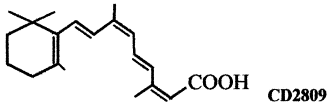 CD2809	RXR

directions with the Kit Dye Terminator Sequencing (PE Applied Biosystem) according to manufacturer's instructions. Ethanol precipitation was performed to eliminate the unincorporated nucleotides. Products of sequencing reactions were analysed with ABI310 sequencer (PE Applied Biosystem).

3. Results

3.1. Effect of RAR selective retinoids on the growth of human glioblastoma cell lines: inhibition of cell proliferation by CD437

The retinoids CD336 (selective for RARα), CD2019 (selective for RARβ), CD666, CD2325, CD437 (selective for RARγ) and CD2809 (selective for RXR) (presented in Table 1) were used at concentrations ranging from 0.1 to 10 μM, and for periods of 24 and 72 h. Fig. 1a shows that the retinoids CD336, CD2019, CD666 and CD2809, at 1 μM for 48 h either had no effect or stimulated cell growth of these cell lines. 8MG-BA cells were less sensitive than GL-15 cells to the strong growth stimulating potential of CD666. In contrast, the two other RARγ agonists CD2325, and to a greater degree CD437, exhibited a growth inhibitory effect on both cell lines. CD2325 only exhibited efficient growth inhibition at higher concentrations (5 and 10 μM) up to 24 h by reducing the levels of [^{3}H]-thymidine incorporation to 45% of control levels in both cell lines (data not shown). As shown in Fig. 1b, inhibition of 8MG-BA cell proliferation by CD437 was concentration- and time-dependent. A single application of 1 μM CD437 induced a growth inhibition of 78% at 24 h, and of 97% at 72 h. At the highest CD437 concentrations (5 and 10 μM), growth inhibition reached 94 and 100% of the control, respectively. In addition, treatment of GL-15 cells with CD437 induced a dose-dependent growth inhibition. Exposure to 1, 5 or 10 μM CD437 for 24 h

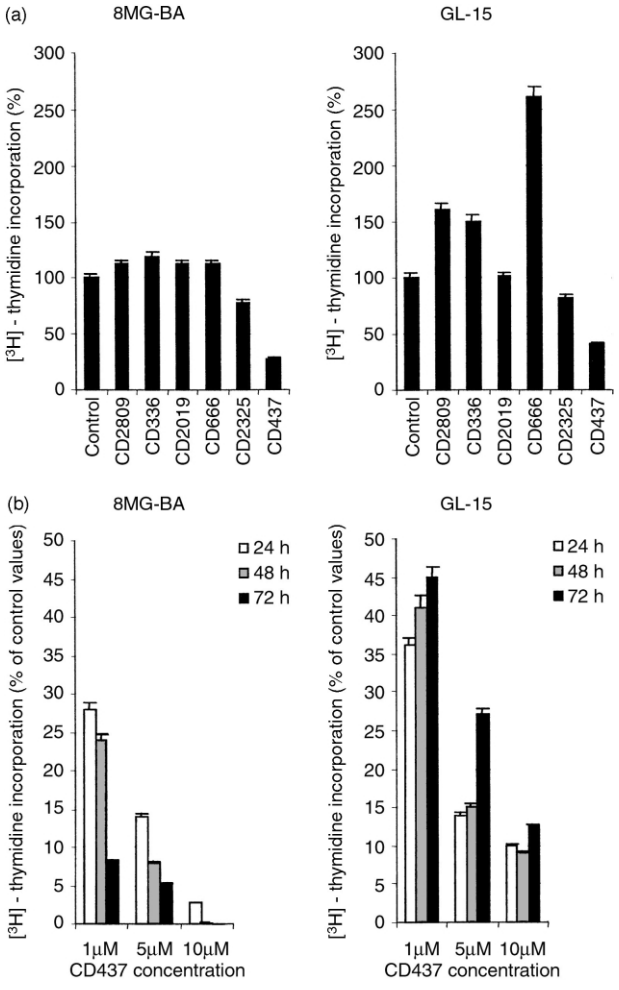

Fig. 1. [^{3}H]-thymidine incorporation into DNA: (a) Effect of various retinoids on the growth of 8MG-BA and GL-15 cell lines treated with 1 μM of the indicated retinoid for 48 h; (b) time- and concentration-dependent growth inhibition in 8MG-BA and GL-15 cells treated with 1, 5 or 10 μM CD437 for 24–72 h. Results are expressed as percentage of [^{3}H]-thymidine incorporation versus control cells. Control cells were treated with vehicle alone. Data are representative and expressed as means±standard error of the mean (SEM) ($n=3$) values.

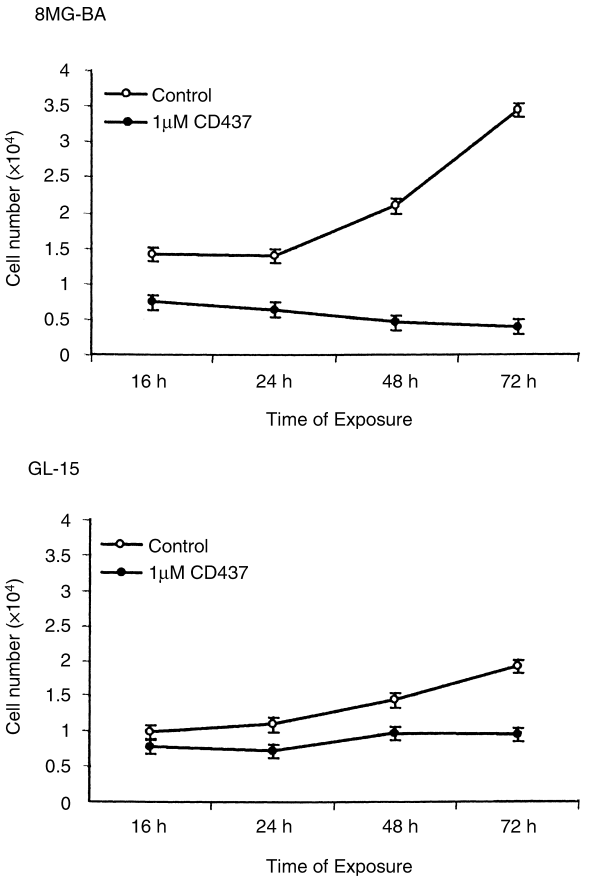

Fig. 2. CD437 inhibition of 8MG-BA and GL-15 cell proliferation. The cells were incubated with 1 μM CD437 and viable cells (excluding Trypan Blue dye) were counted after 16, 24, 48 and 72 h. Control cells were incubated with vehicle alone. The data represent the mean±SEM of three independent experiments.

inhibited proliferation by 64, 86 and 90%, respectively, based on the levels of [^{3}H]-thymidine incorporation.

Interestingly, treatment with 1 μM CD437 reduced the number of viable 8MG-BA and GL-15 cells to 60 and 70%, respectively, at 16 h and the cell numbers were relatively stable over a 72 h period (Fig. 2).

We also analysed the cell cycle distribution by flow cytometry after CD437 treatment. For both cell lines, in the absence of any treatment, the proportion of cells in the G1 phase increased with time, with a concomitant decrease in S phase (data not shown). CD437 induced changes in the cell cycle distribution that varied with the cell line. After 16 h of treatment of 8MG-BA cells with 1 μM CD437, the proportion of cells in G1 phase decreased with a concomitant accumulation of the cells in S phase, while virtually no cells (0.1%) were detected in the G2 phase (Fig. 3c). The number of GL-15 cells also decreased in G1 phase and increased in S phase, but only after 24 h of treatment with 1 μM CD437, and some cells in G2 phase could still be detected (11.1%) (Fig. 3d).

3.2. RAR expression in 8MG-BA and GL-15 cells

In order to evaluate whether the effects of CD473 were related to RAR expression, we analysed the expression of RAR isotypes.

By RT-PCR we observed that both 8MG-BA and GL-15 cells express constitutively the RAR isoforms *RARα2*, *RARβ2*, *RARγ1* and *RARγ2* (Fig. 4). GL-15 cells displayed higher basal levels of *RARα2*, *RARβ2* and *RARγ1* than 8MG-BA cells. Interestingly, in both cell lines CD437 increased the expression of *RARα2* and *RARβ2*, but did not affect the expression of *RARγ1* and *RARα2*.

3.3. CD437-induced apoptosis of glioma cells

In order to determine whether CD437 induces apoptosis in 8MG-BA and GL-15 cells, two independent parameters were chosen: Hoechst 33258 staining and detection of phosphatidylserine on the outer leaflet of apoptotic cell membranes by Annexin V labelling. After

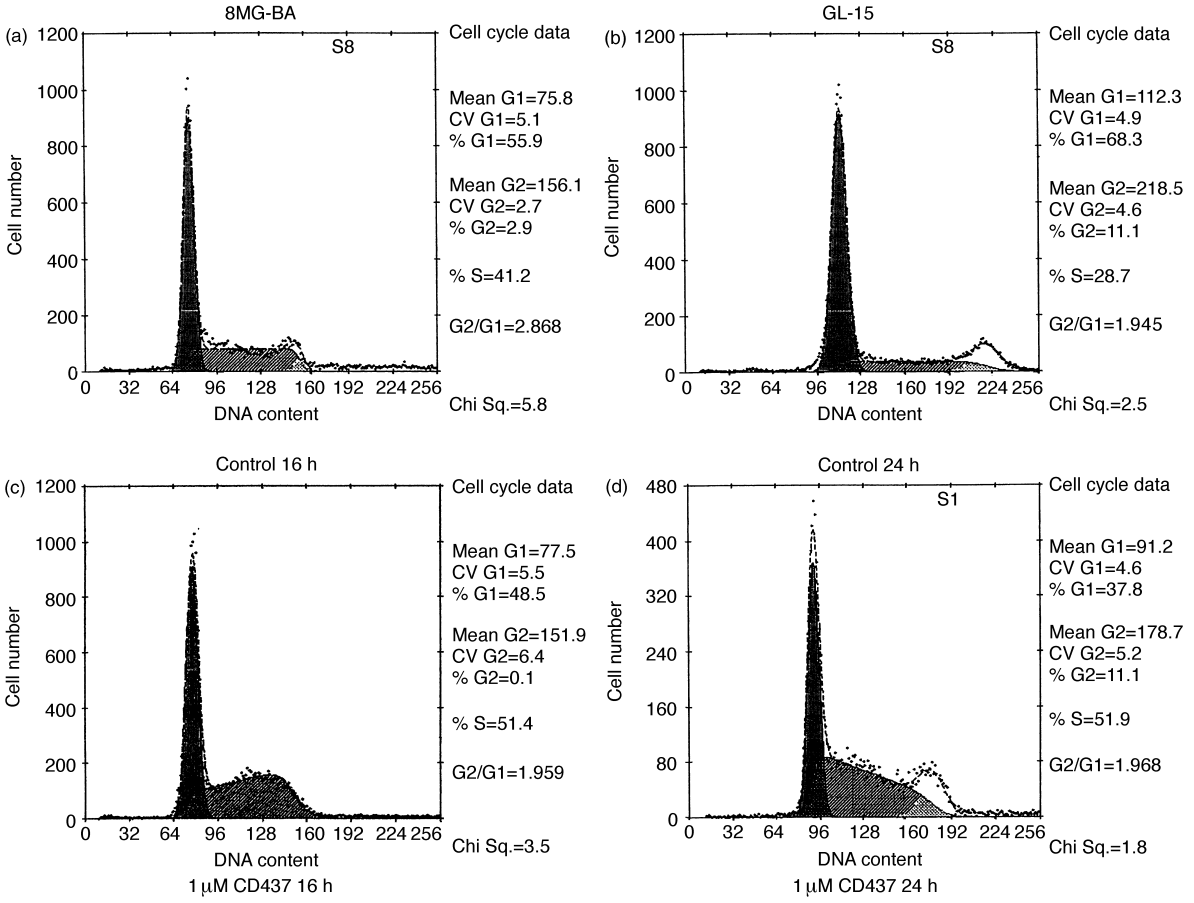

Fig. 3. DNA content analysis by flow cytometry in 8MG-BA and GL-15 human glioblastoma cell lines. Cells were treated with 1 μM CD437 for the indicated times, stained with propidium iodide, and analysed by flow cytometry. The DNA content is presented as relative fluorescence. The number of cells in G0/G1 phase are represented in the first peak, in G2/M phase, in the second peak. Cells in S phase are present in the area between G0/G1 and G2/M peaks.

6 h of treatment with 1 μM CD437, Annexin V staining showed the presence of Annexin V labelling on treated 8MG-BA (Fig. 5A, b) and GL-15 (Fig. 5A, d) cells. Nuclear condensation and fragmentation were observed by Hoechst staining after a 24 h exposure to 1 μM CD437 in approximately 30% of 8MG-BA cells (Fig. 5B, b) and approximately 10% of GL-15 cells (Fig. 5B, d). Altogether, these results indicate that CD437 induces apoptosis in 8MG-BA and GL-15 cells.

Members of the Bcl-2 family are involved in the regulation of the apoptotic process [14]. Therefore, we examined by western blotting, the effect of CD437 on Bcl-2 and Bax protein expression. Fig. 6a shows that Bcl-2 was expressed in both cell lines. The expression of Bcl-2 was inhibited in 8MG-BA cells treated for 16 h with 1 μM CD437. However, Bcl-2 levels were not affected by CD437 in GL-15 cells. Bax was highly expressed in both cell lines, but the levels of this protein were not clearly affected by 1 μM CD437. These data suggest that inhibition of Bcl-2 in 8MG-BA cells may render these cells more susceptible to the apoptotic effect of CD437.

To support the idea that CD437 induces apoptosis in our model and may involve activation of caspases, we measured CPP32-like caspase activity in cytosolic extracts from 8MG-BA and GL-15 cells treated with 1 μM CD437. CPP32 caspase-like activity was increased in 8MG-BA cells after 9 h of treatment, and the addition of the caspase inhibitor z-DEVD-CHO suppressed this effect (Fig. 6b). In contrast, no change in CPP32 caspase-like activity was observed in CD437-treated GL-15 cells.

We also tested whether the effects of CD437 involved *p53* by analysing the *TP53* sequence. A *TP53* mutation in the sequence R273C of exon 8 was detected in the 8MG-BA cells with a substitution of the codon CGT by TGT. In contrast, GL-15 cells presented a deletion of three base pairs located in one allele in exon 5 of the *TP53* gene from the third nucleotide of codon 177. However, preliminary results suggest that both cells

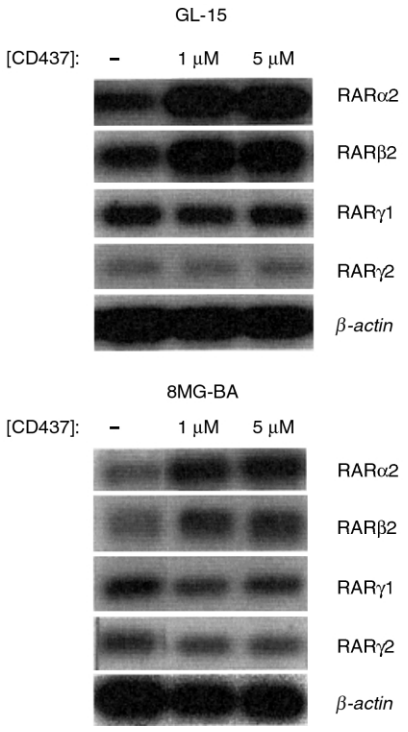

Fig. 4. Reverse transcriptase-polymerase chain reaction (RT-PCR) assays performed on total RNA fractions of 8MG-BA and GL-15 cells exposed to CD437, using specific probes for *RARα2*, *RARβ2*, *RARγ1*, *RARγ2* isoforms and *β-actin*. The RT-PCR blots were probed with end-labelled oligonucleotides probes and analysed by autoradiography.

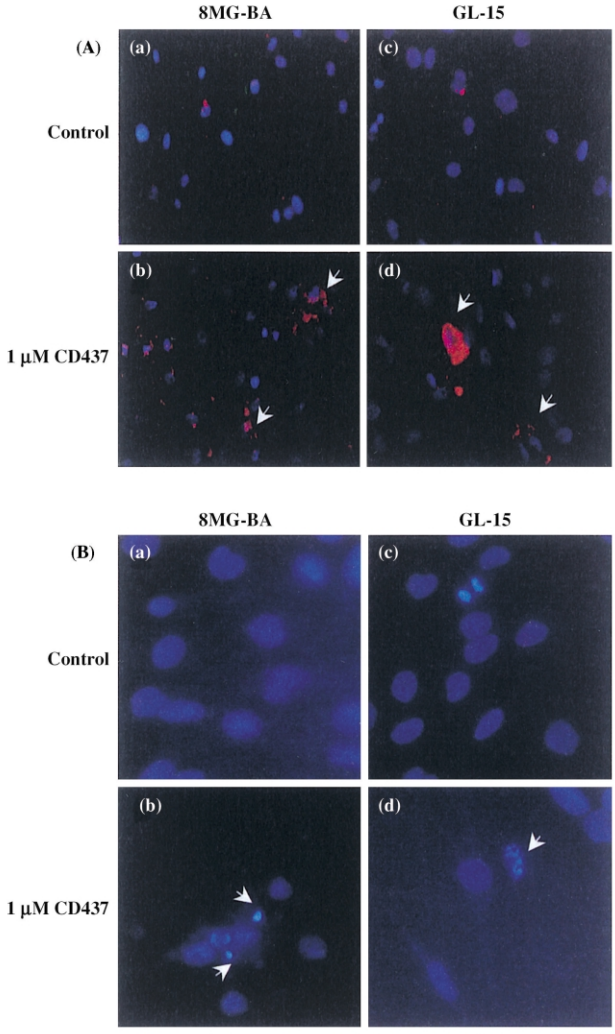

Fig. 5. Induction of apoptosis by CD437 in human 8MG-BA and GL-15 glioblastoma cell lines: (A) identification of phosphatidylserine in the outer leaflet of apoptotic cell-membranes detected by Annexin V binding (arrows) in control conditions or after treatment with 1 μM CD437 for 6 h; (B) morphological analysis of nucleus of 8MG-BA and GL-15 cells in control conditions, and nuclear fragmentation detection by Hoechst 33258 dye in cells treated with 1 μM CD437 for 24 h. Arrows represent apoptotic bodies and fragmented nuclei.

lines express p53 protein constitutively. In addition, p53 protein levels were increased by CD437 in both cell lines (data not shown).

3.4. CD437 potential to induce differentiation of glioma cells

Immunolabelling of vimentin and GFAP showed that confluent control 8MG-BA cells had a spread out, polygonal shape and expressed high vimentin and low GFAP levels (Fig. 7a and b, respectively). Confluent control GL-15 cells had a bipolar shape with high vimentin and heterogeneous GFAP expression (Fig. 7e and f, respectively). After 24 h of treatment with 1 μM CD437, the remaining 8MG-BA cells presented phenotypic changes, illustrated by a condensed cell body and formation of long thin processes, and an increase in GFAP immunolabelling (Fig. 7c and d, respectively). In contrast, a proportion of the remaining GL-15 cells presented a bipolar, multiprocessed phenotype with higher levels of GFAP expression (Fig. 7g and h, respectively). Western blot analysis showed that control GL-15 cells expressed higher GFAP levels than 8MG-BA cells (Fig. 8). However, GFAP protein increased in both cell lines after a 24 h exposure to 1 μM CD437. A parallel increase in GS levels, a protein involved in the metabolism of mature astrocytes, was also observed under these conditions. In contrast, steady-state vimentin levels remained unchanged.

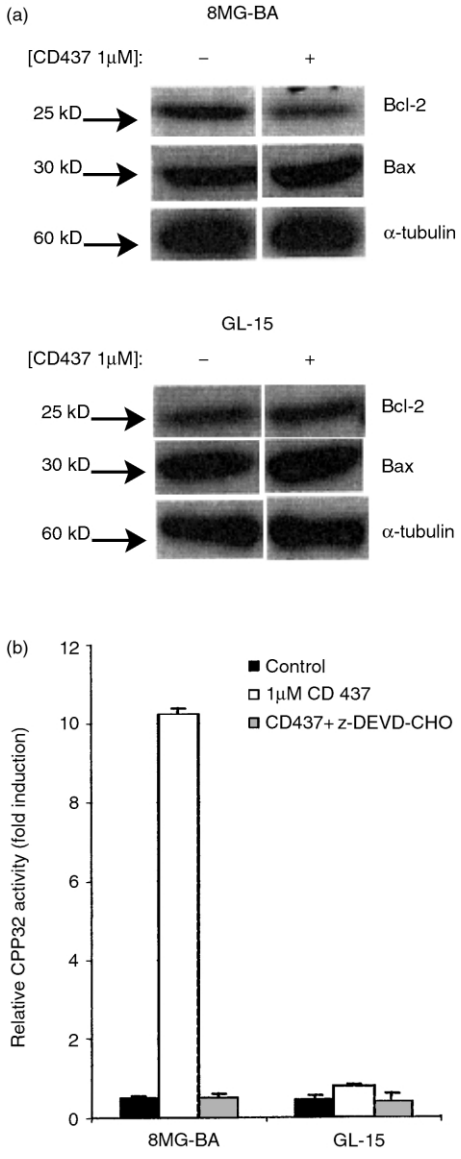

Fig. 6. Effect of CD437 on Bcl-2 and Bax expression, and on CPP32 activation in human glioblastoma cell lines. (a) Cells extracts were prepared from 8MG-BA and GL-15 cells treated with 1 μM CD437 for 16 h and analysed by western blot for the expression of Bcl-2 and Bax. Expression of α-tubulin was used as a control. (–, not treated with CD437). The data represent one independent experiment of three. (b) CPP32 caspase-3-like activity in 8MG-BA and GL-15 cells in control conditions, or treated with 1 μM CD437 alone or in combination with CPP32 inhibitor Z-DEVD-CHO for 9 h. These results are representative of three independent experiments.

4. Discussion

Malignant gliomas are highly invasive, rapidly proliferating tumours [15] and present a poor prognosis. Unfortunately, the most aggressive conventional treatments for these tumours are still associated with short survival [16,17].

In this study, we demonstrated that treatment of exponentially dividing 8MG-BA [13] and GL-15 [18] human glioblastoma cells with CD437, described as a RARγ agonist [19], causes strong inhibition of cell proliferation and induces apoptosis. This contrasts with reports on other selective agonists of retinoid acid receptor subtypes RARα (CD336), RARβ (CD2019), RARγ (CD2325 and CD666) and RXR (CD2809).

CD437-induced apoptosis was rapid and growth arrest was characterised by the accumulation of the cells in the S phase of the cell cycle. Such an accumulation in S phase was recently mentioned as a result of CD437 treatment of lymphomas [20] and human non-small cell lung carcinoma cells [21]. Interestingly, breast cancer and lung carcinoma cells also underwent apoptosis when treated with CD437, but these cells arrested in the G0/G1 phase of the cell cycle [8,10]. The question as to why CD437 causes growth arrest at different stages of the cell cycle depending on the cell type has not been elucidated. It has been demonstrated that persistent DNA damage inhibits DNA replication and S-phase progression and subsequently activates apoptotic pathways [22]. Thus, the inability of the cells to incorporate [^{3}H]-thymidine upon CD437 exposure could be explained by DNA damage present during S phase which could overwhelm the capacity of the repair mechanisms.

Although the binding of retinoids to their receptors seems to be a prerequisite for their biological activities, we found no correlation between the receptor subtype-binding activity and the growth-inhibitory effects of retinoids. Of all the retinoids tested, CD437 and CD2325, two structurally-related RARγ agonists, were the most potent molecules to inhibit the proliferation of 8MG-BA cells, whereas CD666, another RARγ-selective retinoid, was not effective, and even induced cell proliferation in the GL-15 cell line. In both 8MG-BA and GL-15 cells, CD437 activates the expression of RA-responsive genes, such as those coding for RARα2 and RARβ2. Thus, it can be suggested that upon induction of these receptors, genes involved in the regulation of the cell cycle are activated, leading to cell growth arrest. In that respect, RARβ2 has recently been shown to be required for the growth inhibitory action of RA [23]. Our preliminary *in vitro* observations also suggest that

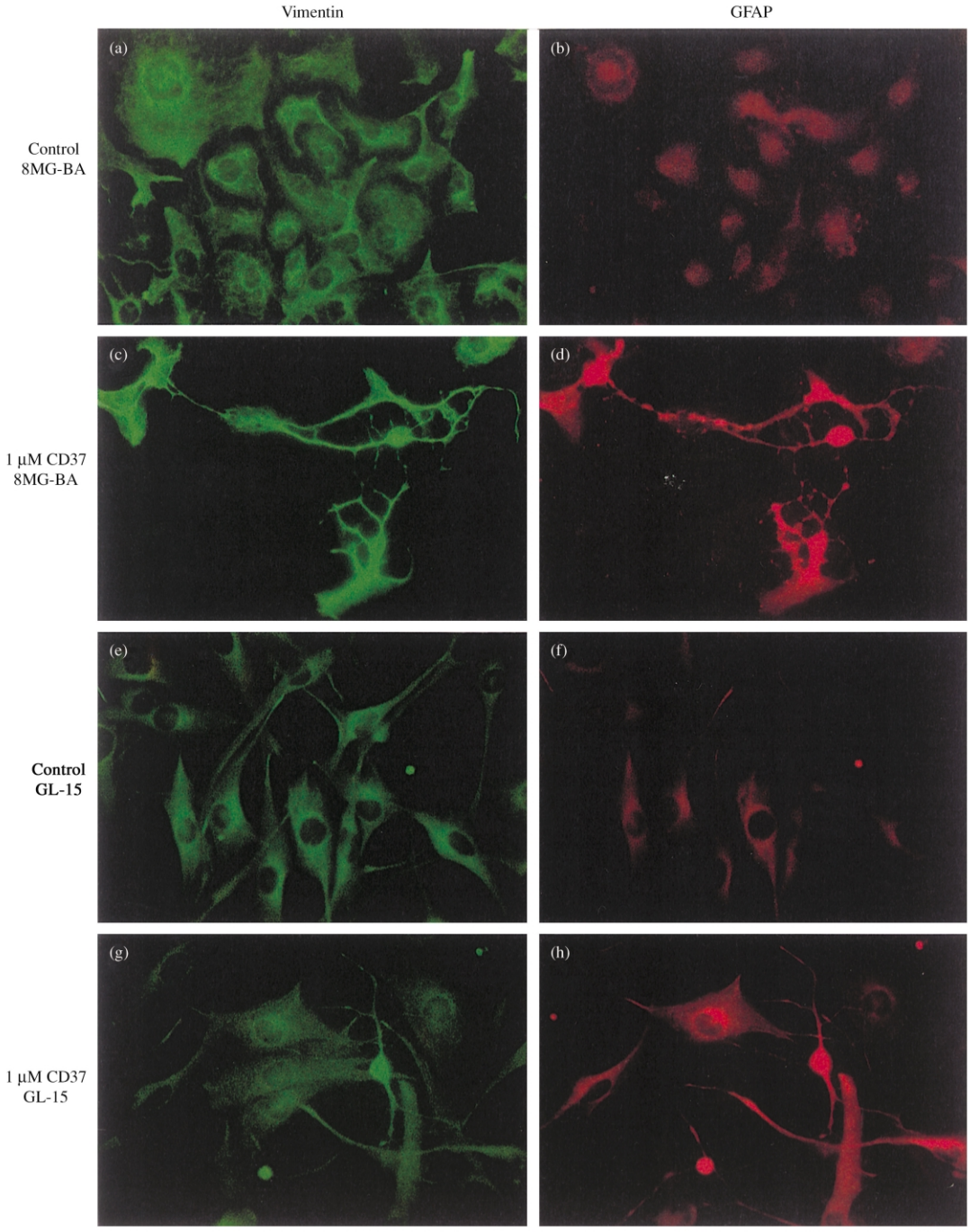

Fig. 7. Immunofluorescence labelling of glial fibrillary acidic protein (GFAP) and vimentin in 8MG-BA (a–d) and GL-15 cells (e–h) grown in control conditions or treated with 1 μM CD437 for 24 h.

RARβ agonists might be involved in both growth arrest and glioma cell differentiation (data not shown). In addition, CD437 was recently reported to exert its effects on cell growth and differentiation through RARs. In contrast, the induction of apoptosis by this compound would seem to be RAR-independent [24].

In the present work, we provide evidence that CD437 rapidly induces apoptosis in 8MG-BA and GL-15 cells, as indicated by Annexin V labelling and DNA fragmentation. Apoptosis is a complex, multistage process involving many genes such as *TP53* [25]. However, in breast carcinoma cells, CD437-induced apoptosis does not require p53 [10]. Moreover, in the present case, although 8MG-BA and GL-15 glioblastoma cell lines displayed *TP53* gene abnormalities, both cell lines expressed the p53 protein and overexpressed it upon CD437 treatment (data not shown). These preliminary results suggest the *TP53* gene may be CD437 target and the induced cascade of events should be investigated. The higher sensitivity of 8MG-BA cells to CD437 cannot be correlated with p53 expression. In order to further probe the mechanism by which CD437 induces apoptosis of glioblastoma cells, we examined the expression of two proteins that have been described as being involved in the apoptotic pathway, Bcl-2 and Bax. Bcl-2 is an oncoprotein known to inhibit apoptosis or induce cell survival in a variety of cell types [26–28]. Bcl-2 homodimerises or heterodimerises with a number of other proteins, including Bax [27], and Bax has been shown to promote apoptosis. It has been suggested that it is not the level of Bcl-2 *per se*, but the ratio between members of this protein family, that is a critical factor in regulating apoptosis [28,29]. According to our results, Bcl-2 would be one factor contributing to the sensitivity of glioblastoma cells to the induction of apoptosis by CD437, and since it is inhibited in CD437-treated 8MG-BA cells, these undergo rapid apoptosis. However, as our results suggest, such a role for Bcl-2 might be cell-type specific, since CD437 induces apoptosis in GL-15 cells without affecting Bcl-2 levels. Thus, the ultimate biochemical mechanisms and effectors of apoptotic cell death triggered by CD437 still remain elusive. Current evidence indicates that proteases, known as caspases, could be central components of the cell death machinery in various forms of apoptosis. Among the 10 members of caspases thus far identified, CPP32 is one of the strongest candidates. Indeed, CPP32 is a mammalian cell-death-inducing protease that cleaves poly (adenosine-diphospho-ribose (ADP)-ribose) polymerase, a nuclear enzyme involved in DNA repair and maintenance of the genome and protein integrity [29]. Its activation by CD437 in acute promyelocytic leukaemia cells supports this concept [9]. Our results also support this concept, since CPP32 activity is rapidly induced in 8MG-BA cells. However, this caspase was not affected in GL-15 cells. These results indicate that activation of this protease is involved in the apoptosis induced by CD437 in 8MG-BA cells, but not in GL-15 cells.

After 24 h of CD437 exposure, we also observed that the majority of the surviving 8MG-BA cells, and a significant number of the remaining GL-15 cells, underwent astroglial differentiation. These cells presented an astroglial phenotype with many filamentous processes and cytoplasmic retraction. This differentiation potential of CD437 was confirmed by the overexpression of two known markers of astroglial differentiation: the glial fibrillary acidic protein (GFAP) and glutamine

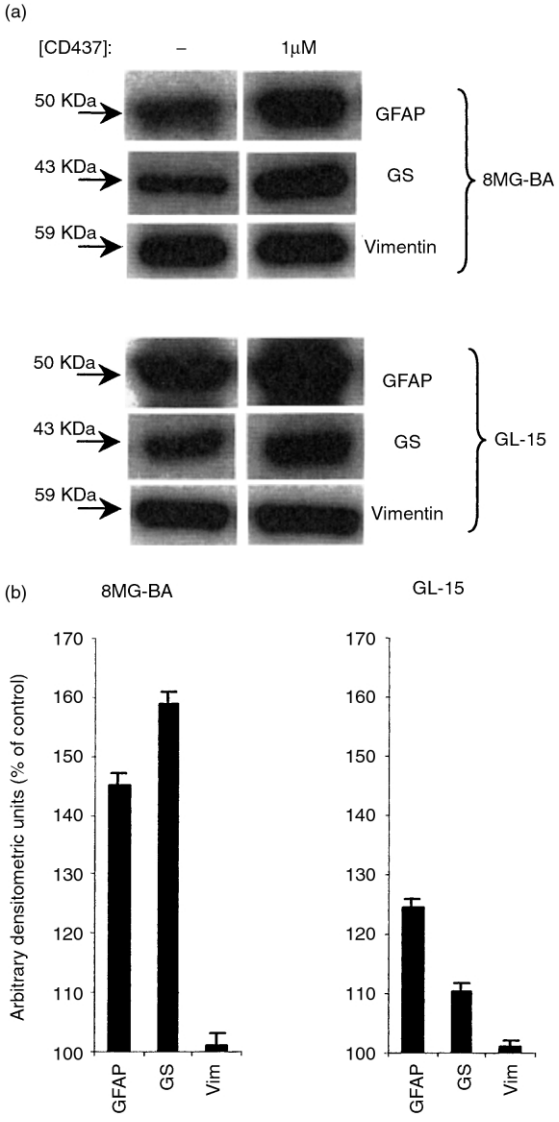

Fig. 8. Modulation of glial fibrillary acidic protein (GFAP) and glutamine sytnetase (GS) expression by CD437 in human glioblastoma cell lines. (a) Western blot of cell extracts from 8MG-BA and GL-15 cells in control conditions or treated with 1 μM CD437 for 24 h; (–, not treated with CD437). (b) Histograms represent the relative expression of GFAP, GS and vimentin in both cell lines. Data are representative of three individual experiments and are expressed as means±standard error of the mean (SEM). Vim, vimentin.

synthetase (GS). Studies have reported that GFAP is related to differentiation in malignant gliomas [30,31] and GS has been reported as an astroglial metabolic maturation marker [32–34]. These observations prompted us to conclude that CD437 has a dual potential, induction of apoptosis and triggering of the remaining non-apoptotic cells towards a differentiated phenotype.

In conclusion, we assert that CD437 induces either Bcl-2 and CPP32-dependent or independent apoptosis in human glioblastoma cells, depending on the cell line. CD437 also induces growth arrest and differentiation of glioblastoma cells, as illustrated by cytoskeletal restructuring and metabolic maturation of non-apoptotic cells. Thus, our data support the idea that CD437 may find clinical applications in the treatment of glioblastoma through a mechanism of activation which seems to be substantially different from that of t-RA, thus such compound may find a special application in the treatment of t-RA-resistant relapses.

Acknowledgements

The authors gratefully acknowledge Dr Uwe Reichert (*Galderma*, Sophia Antipolis, France) for providing the synthetic retinoids, Dr P. Laurent-Puig and Mrs A.M. Houiller (Laboratoire de Toxicologie Moléculaire INSERM U-490, Paris, France) for their collaboration and Dr Suzan Michelson for reading the manuscript. S.L. Costa is recipient of a fellowship from Universidade Federal da Bahia (UFBA) and Fundação Coordenação de Aperfeiçoamento de Pessoal de Nível Superior (CAPES).

References

1. Defer GL, Adle-Biassette H, Ricolfi F, *et al*. All-trans retinoic acid in relapsing malignant gliomas: clinical and radiological stabilization associated with the appearance of intratumoral calcifications. *J Neuro-Oncol* 1997, **34**, 169–177.
2. Chambaut-Guérin AM, Costa SL, Lefrançois T, Fages C, Gauthereau TM. Effect of retinoic acid and tumor necrosis factor alpha on GL-15 glioblastoma cells. *Neuroreport* 2000, **2**, 389–393.
3. De Luca LM. Retinoids and theirs receptors in differentiation, embryogenesis, and neoplasia. *FASEB J* 1991, **5**, 2924–2933.
4. Lotan R. Cellular biology of retinoids. In Degos L, Parkinson DR, eds. *Retinoids in Oncology*. Berlin, Springer-Verlag, 1995, 27–42.
5. Chambon P. A decade of molecular biology of retinoic acid receptors. *FASEB J* 1996, **10**, 940–954.
6. Lehmann JM, Dawson MI, Hobbs PD, Husmann M, Pfhal M. Identification of retinoids with nuclear receptor subtype selective activities. *Cancer Res* 1991, **52**, 4804–4809.
7. Schadendorf D, Kern MA, Artuc M, *et al*. Treatment of melanoma cells with the synthetic retinoid AHPN/CD437 induces apoptosis via activation of AP-1 in vitro, and causes growth inhibition in xenografts in vivo. *J Cell Biol* 1996, **135**, 1889–1898.
8. Li Y, Lin B, Agadir A, *et al*. Molecular determinants of AHPN (CD437)-induced growth arrest and apoptosis in human lung cancer cell lines. *Mol Cell Biol* 1998, **18**, 4719–4731.
9. Mologni L, Ponzanelli I, Bresciani F, *et al*. The novel synthetic retinoid 6-[3-(1-adamantyl)-4-hydroxyphenil]-2-naphthalene carboxylic acid (CD437) causes apoptosis in acute promyelocytic leukemia cells through rapid activation of caspases. *Blood* 1999, **93**, 1045–1061.
10. Shao Z-M, Dawson MI, Li XS, *et al*. p53 independent G0/G1 arrest and apoptosis induced by a novel retinoid in human breast cancer cells. *Oncogene* 1995, **11**, 493–504.
11. Lu XP, Fanjul A, Picard N, *et al*. Novel retinoid-related molecules as apoptosis and effective inhibitors of human lung cancer cells in vivo. *Nat Med* 1997, **3**, 686–690.
12. Bocchini V, Casalone R, Collini P, Rebel G, Curto LF. Changes in GFAP and caryotype during culturing of two cell lines established from human glioblastoma multiforma. *Cell Tiss Res* 1991, **265**, 73–81.
13. Perzelova A, Macikova I, Mraz P, Bizik I, Steno J. Characterization of two permanent glioma cell lines 8MG-BA and 42-MG-BA. *Neoplasma* 1998, **45**, 25–29.
14. Korsmeyer SJ. Regulators of cell death. *Trends Genet* 1995, **11**, 101–105.
15. Bienart W, Tohma Y, Yonekawa Y, Kleihues P, Ohgaki H. Alterations of cell cycle regulatory genes in primary (de novo) and secondary glioblastomas. *Acta Neuropathol* 1997, **94**, 303–309.
16. Fine HA, Dear KG, Loeffler JS, Black PMcL, Canellos GP. Meta-analysis of radiation therapy with and without adjuvant chemotherapy for malignant gliomas in adults. *Cancer* 1993, **71**, 2585–2597.
17. Hildebrand J, Dewitte O, Dietrich PY, Tribolet N. Management of malignant brain tumors. *Eur Neurol* 1997, **38**, 238–253.
18. Arcuri C, Bocchini V, Guerrieri FC, Tardy M. PKC activation induces opposite GFAP expression and morphology in glioblastoma multiforme cell line of clonal origin. *J Neurosc Res* 1995, **40**, 622–631.
19. Bernard BA, Bernardon J-M, Delescluse C, *et al*. Identification of synthetic retinoids with selectivity for human nuclear retinoic acid receptor γ. *Biochem Biophys Res Commun* 1992, **186**, 977–983.
20. Adachi H, Preston G, Harvat B, Dawson MI, Jetten AM. Inhibition of cell proliferation and induction of apoptosis by the retinoid AHPN in human lung carcinoma cells. *Am J Respir Cell Mol Biol* 1998, **18**, 323–333.
21. Sun S-Y, Yue P, Shroot B, *et al*. Differential effects of synthetic nuclear retinoid receptor-selective retinoids on the growth of human non-small cell lung carcinoma cells. *Cancer Res* 1997, **57**, 4931–4939.
22. Orren DK, Petersen LN, Bohr VA. Persistent damage inhibits S-phase and G2 progression, and results in apoptosis. *Mol Biol Cell* 1997, **8**, 1129–1142.
23. Faria TN, Mendelsohn C, Chambon P, Gudas LJ. The target disruption of both alleles of RARβ2 in F9 cells results in the loss of retinoic acid-associated growth arrest. *J Biol Chem* 1999, **74**, 26783–26788.
24. Sun S-Y, Yue P, Mao L, *et al*. Identification of receptor-selective retinoids that are potent inhibitors of growth of human head and neck squamous cell carcinoma cells. *Clinical Can Res* 2000, **6**, 1563–1573.
25. Elledge R, Lee WH. Life and death by p53. *Bio Assays* 1995, **17**, 923–930.
26. Reed JC. Bcl-2 and regulation of programmed cell death. *J Cell Biol* 1994, **124**, 1–6.
27. Boise LH, Gottschalk AR, Quintans J, Thompson CB. Bcl2 and Bcl2-related proteins in apoptosis regulation. *Curr Top Microbiol Immunol* 1995, **200**, 107–121.
28. White E. Life, Death, and the pursuit of apoptosis. *Genes Dev* 1996, **10**, 1–15.
29. De Murcia JM, Niedergang C, Trucco C, *et al*. Requirement of poly (ADP-ribose) polymerase in recovery from DNA damage in mice and in cells. *Proc Natl Acad Sci USA* 1997, **94**, 703–707.

30. Rutka JT, Smith SL. Transfection of human astrocytoma cells with glial fibrillary acidic protein complementary DNA: analysis of expression, proliferation, and tumorigenicity. *Cancer Res* 1993, **53**, 3519–3526.
31. Rutka JT, Hubbard SL, Fukuyama K, Matsuzawa K, Dirks PB, Becker LE. Effects of antisense glial fibrillary acidic protein complementary DNA on growth, invasion, and adhesion of human astrocytomes cells. *Cancer Res* 1994, **54**, 3267–3272.
32. Fages C, Rolland B, Dias Costa MF, *et al*. Messenger RNA coding for glutamine synthetase in cerebral hemispheres and astroglial cultures from mouse brain: a developmental study. *Neurochem Int* 1988, **12**, 307–313.
33. Vardimon L, Ben-Dror I, Havazelet N, Fox LE. Molecular control of glutamine synthetase expression in the developing retina tissue. *Dev Dyn* 1993, **196**, 276–282.
34. Letournel-Boulland ML, Fages C, Rolland B, Tardy M. Lipopolysaccharides (LPS), up-regulate the IL-1-mRNA and down-regulate the glial fibrillary acidic protein (GFAP) and glutamine synthetase (GS)-mRNAs in astroglial primary cultures. *Eur Cytokine Netw* 1994, **5**, 51–56.
35. Taneja R, Rochette-Egly C, Plassal J-L, Penne L, Ilfaub M-P, Chambon P. Phosphorylation of activation functions AF-1 and AF-2 of RARα and RARγ is indispensible for differentiation of F9 cells upon retinoic acid and cAMP treatments. *EMBO J* 1997, **16**, 6452–6465.